Apatite-forming ability of glass-ceramic apatite–wollastonite – polyethylene composites: effect of filler content

J. A. JUHASZ*, S. M. BEST, W. BONFIELD
Department of Materials Science and Metallurgy, University of Cambridge, UK
E-mail: jaj33@cam.ac.uk

M. KAWASHITA, N. MIYATA, T. KOKUBO
Department of Material Chemistry, Graduate School of Engineering, Kyoto University, Japan

T. NAKAMURA
Department of Orthopaedic Surgery, Graduate School of Medicine, Kyoto University, Japan

The bioactivity of a range of glass-ceramic apatite–wollastonite (A–W) – polyethylene composites (AWPEXs) with glass-ceramic A–W volume percentages ranging from 10 to 50, has been investigated in an acellular simulated body fluid (SBF) with ion concentrations similar to those of human blood plasma. The formation of a biologically active apatite layer on the composite surface after immersion in SBF was demonstrated by thin-film X-ray diffraction (TF-XRD) and field-emission scanning electron microscopy (FE-SEM). An apatite layer was formed on all the composites, with the rate of formation increasing with an increase in glass-ceramic A–W percentage. For composites with glass-ceramic A–W filler contents $\geq$ 30 vol %, the apatite layer was formed within 12 h of immersion, which is a comparable time for apatite formation on monolithic glass-ceramic A–W. Inductively coupled plasma atomic emission spectroscopy (ICP-AES) demonstrated that the apatite formation on AWPEX samples with 50 vol % filler content occurred in a manner similar to that seen on pure glass-ceramic A–W, in that the calcium, silicon, and magnesium ion concentrations increased and, conversely, a decrease was observed in the phosphate ion concentration. These results indicate that a suitable *in vitro* response was achieved on a composite incorporating particulate glass-ceramic A–W with a particularly favorable response being observed on the AWPEX sample with 50 vol % filler content.

1. Introduction

In 1982, Kokubo *et al*. [1] developed glass-ceramic A–W containing crystalline apatite ($Ca_{10}(PO_4)_6(O,F_2)$) and wollastonite ($CaO \cdot SiO_2$) in a $MgO–CaO–SiO_2$ glassy matrix. This glass–ceramic has mechanical strength superior to both Bioglass® and sintered hydroxyapatite [2–5], as well as human cortical bone [6, 7]. Since its discovery, glass-ceramic A–W has widely been used as a bone substitute in applications such as iliac crest prostheses and artificial vertebrae due to its high bioactivity and the ability to bond spontaneously to living bone without the formation of a fibrous layer [8, 9]. The superior mechanical performance of glass-ceramic A–W can be maintained for a long period in the body environment, making it a highly desirable implant material [10, 11]. However, glass-ceramic A–W has a relatively low fracture toughness, which makes it unsuitable for major load-bearing applications such as in the femoral and tibial bones. It is also difficult for a surgeon to readily shape the material with a scalpel prior to implantation, which would be particularly useful when the volume of the implant needs to be altered to fit precisely the volume of bone which it is to replace.

Following the success of HAPEX™ (hydroxyapatite–polyethylene composite) as an implant material [12–15] and, in an attempt to widen the use of glass-ceramic A–W so as to take advantage of its high stiffness and bioactivity, a composite was created incorporating glass-ceramic A–W in a matrix of polyethylene. Preliminary studies have already shown this composite to possess promising mechanical properties [16]. In the present study, the bioactivity was analyzed by immersion into SBF with ion concentrations almost equal to those of human blood plasma, since it has been proven to be able to produce an apatite layer on glass-ceramics and glasses [17]. Composites were created using five different glass-ceramic A–W filler contents; 10–50 vol %. The formation of a bone-like apatite on the surface of each composite was evaluated in SBF at a constant temperature of 36.5 °C, so as to identify the most

* Author to whom all correspondence should be addressed.

suitable compositions for potential implant applications. The change in calcium, phosphate, magnesium and silicon ion concentration during apatite formation was evaluated by inductively-coupled plasma atomic emission spectroscopy (ICP-AES) to assist in this selection.

2. Experimental procedure

2.1. Materials

Glass-ceramic A–W (supplied by Nippon Electric Glass Co. Ltd., Japan) was incorporated into high-density polyethylene (Rigidex HM4560XP, BP Chemicals Ltd., UK) by twin screw extrusion and compression molding [18]. The glass-ceramic A–W filler content was set at 10, 20, 30, 40, and 50 vol % (the composites being denoted as AWPEX-10, -20, -30, -40, and -50). HAPEX™ (filler content set at 40 vol %) was also produced as a comparison with the AWPEX samples.

The amount of each component needed in AWPEX and HAPEX™ was calculated from the following equations:

$$\mathrm{wt}_F\,(g) = \frac{(\mathrm{vol}\,\%_F \times \rho_F)}{(\mathrm{vol}\,\%_F \times \rho_F) + (\mathrm{vol}\,\%_M \times \rho_M)} \times 1000\,(\text{in order to convert to grams})$$

$$\mathrm{wt}_M\,(g) = \frac{(\mathrm{vol}\,\%_M \times \rho_M)}{(\mathrm{vol}\,\%_F \times \rho_F) + (\mathrm{vol}\,\%_M \times \rho_M)} \times 1000$$

where subscript F denotes glass-ceramic A–W or hydroxyapatite, M denotes polyethylene, wt is the weight in grams, and ρ is the density of A–W or PE, taken as $3.07\,\mathrm{mg\,m^{-3}}$ and $0.94\,\mathrm{mg\,m^{-3}}$, respectively.

Prior to processing, the glass-ceramic A–W powder was characterized in terms of size and morphology using a laser scattering particle size distribution analyzer (LA-700S, Horiba Co., Japan) and a field-emission scanning electron microscope (FE-SEM: S-4700, Hitachi, Japan). Hydroxyapatite (HA) powder used in HAPEX™ was also evaluated for comparison. Before FE-SEM analysis, the powders were dried fully and then sprinkled onto a metal stub onto which carbon adhesive had been placed. Excess powder was gently removed using an air duster. The stubs with attached powders were vacuum-sealed into a coating chamber and coated with Au–Pd for 3–4 min. During FE-SEM analysis, an accelerating voltage of 15 kV and a working distance of 12 mm were used.

2.2 Bioactivity

Samples of dimensions $2 \times 10 \times 10\,\mathrm{mm^3}$ were created from the compression molded plates of AWPEX, as well as pure glass-ceramic A–W, pure high-density polyethylene (HDPE) and HAPEX™. All samples were ground to an 8 μm finish with silicon carbide paper and then washed in ethanol in an ultrasonic bath. The samples were then allowed to dry fully. Each batch was soaked in 30 ml of simulated body fluid (SBF) [17] at 36.5 °C with pH and ionic concentrations nearly equal to those in human blood plasma (Table I). At periodic intervals, the specimens were removed from the solution, washed with distilled water to remove excess SBF, and then allowed to air dry. The surfaces were analyzed using thin-film X-ray diffractometry (TF-XRD: RINT-2500, Rigaku Co., Japan) and FE-SEM before and after soaking in SBF. The TF-XRD measurement was performed using CuK_α ($\lambda = 0.15405\,\mathrm{nm}$) radiation as the source, at a rate of $2\theta = 2^\circ/\mathrm{min}$ and a glancing angle of 1° against the incident beam on the composite surface.

TABLE I Table showing ionic concentrations and pH of simulated body fluid in comparison to human blood plasma

Ion	Concentration (mM)	
	Human blood plasma	Simulated body fluid
Na^+	142.0	142.0
K^+	5.0	5.0
Mg^+	1.5	1.5
Ca^{2+}	2.5	2.5
Cl^-	103.8	147.8
HCO_3^-	27.0	4.2
HPO_4^{2-}	1.0	1.0
SO_4^{2+}	0.5	0.5
pH	7.20–7.40	7.40

2.3. ICP-AES analysis

Samples of AWPEX-30, -40, -50, as well as pure glass–ceramic A–W and HAPEX™, were cut and polished to a size of $2 \times 10 \times 10\,\mathrm{mm^3}$. Final polishing of all the samples was performed using 8 μm silicon carbide paper. The specimens were then soaked in 30 ml of SBF with pH 7.40 at 36.5 °C for up to 14 days.

The changes in the elemental concentrations (calcium, phosphate, magnesium, and silicon ions) of the SBF after immersion of the most bioactive composites (AWPEX-30, -40, and -50 in comparison to pure glass-ceramic A–W and HAPEX™, were measured using ICP-AES (Model SPS1500, Seiko Inst., Japan).

3. Results

The as-received glass-ceramic A–W powder showed a broad size distribution, with a median particle size of 4.38 μm. The HA particle size distribution was narrower and the median particle size was 3.42 μm (Fig. 1). Both the powders had significant amounts of sub-microscopic sized particles. While the hydroxyapatite particles demonstrated smooth surfaces at a sub-microscopic level (Fig. 2(b)) with nodular protrusions of ≈ 0.5 μm, the glass-ceramic A–W particles possessed a smooth surface, but with angular surfaces on a macroscopic scale (Fig. 2(a)). After compounding, the particles in both HAPEX™ and AWPEX were observed to be well-dispersed in a homogeneous distribution within the polymer matrix.

Fig. 3 shows the TF-XRD patterns of the surface of the composites after soaking in SBF, as well as that of the untreated specimens. The peaks ascribed to apatite and wollastonite were observed for all AWPEX samples. For HAPEX™, the peaks for apatite were present (Fig. 3). A large peak for PE was seen for all the composite samples, as well as pure HDPE prior to immersion in SBF. After only 3 h of treatment, a decrease was observed in the PE peaks for all the composites with 30 vol % or greater filler content. At this point, no change was observed for pure PE, as expected, due to its ''inert'' nature, and the

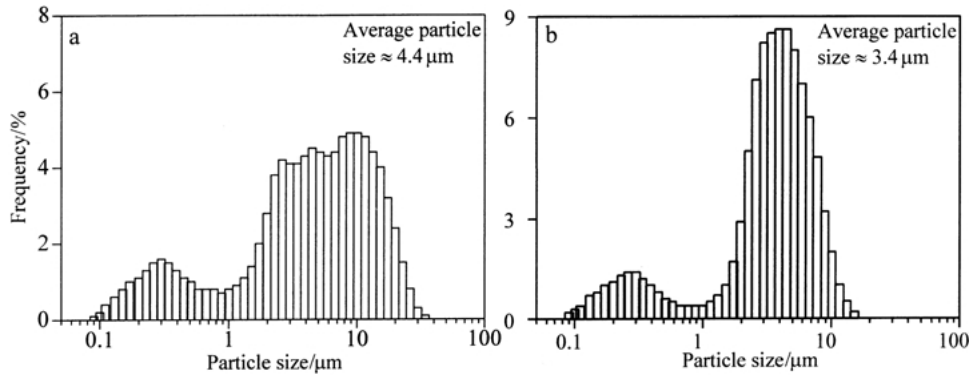

Figure 1 Particle size distribution of filler powders. Glass-ceramic A–W (a) and HA (b).

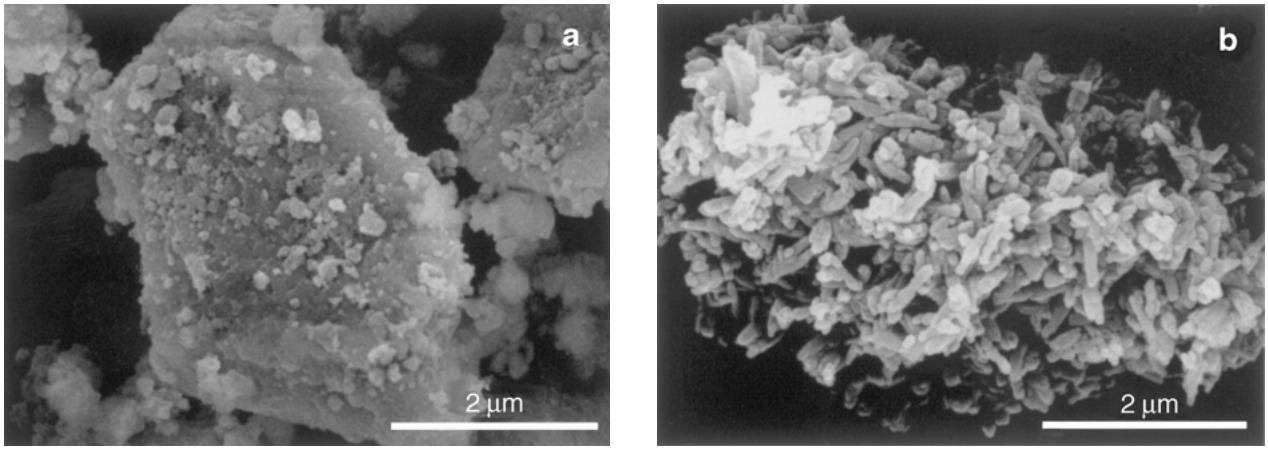

Figure 2 FE-SEM showing morphologies of glass–ceramic A–W (a) and HA (b) powders.

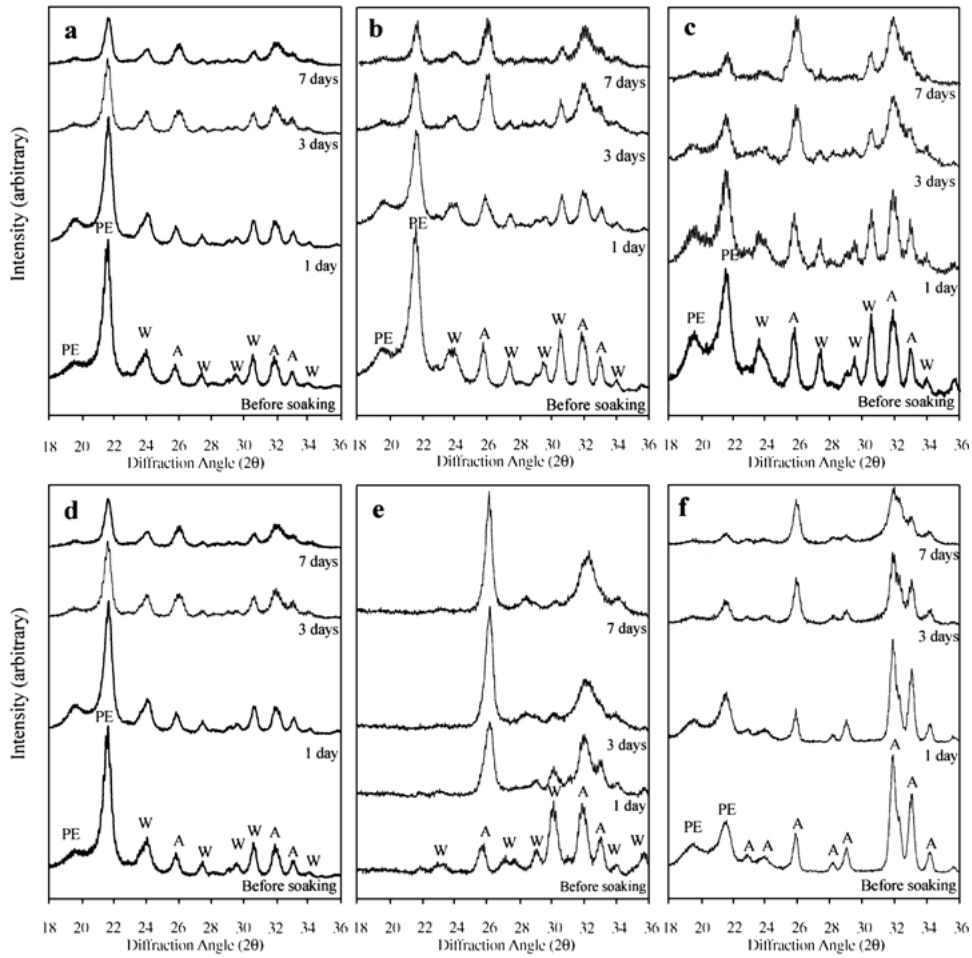

Figure 3 TF-XRD traces for AWPEX, glass-ceramic A–W and HAPEX^{TM} samples before and after soaking in SBF; AWPEX-20 (a), AWPEX-30 (b), AWPEX-40 (c), AWPEX-50 (d), glass-ceramic A–W (e), and HAPEX^{TM} (f). A = apatite, W = wollastonite and PE = polyethylene.

AWPEX samples with 10 and 20 vol % filler content. A decrease in the major wollastonite peak was also observed, in the case of AWPEX samples. A sharp decrease in both these crystalline phases was observed between 12 h and 1 day for the AWPEXs with filler contents ≥ 30 vol %. In addition to the decrease in wollastonite and polyethylene that were detected, a gradual increase in apatite was observed both in the TF-XRD and FE-SEM results for all composites. With increasing filler content, the increase in the apatite peaks was more pronounced at an earlier stage of immersion. After just 1 day immersion the AWPEXs with filler contents 30, 40, and 50 vol %, and HAPEX™ all had a bioactive layer of apatite covering their entire surfaces. However, it took 3 days for the same degree of coverage to be achieved on the AWPEX samples with 10 and 20 vol % filler content. The coverage of apatite on HAPEX™ after 1 day consisted mainly of apatite nuclei and less growth of these sites compared to AWPEX-40. The FE-SEM image (Fig. 4) shows these growths on HAPEX™ at a higher magnification than on pure glass-ceramic A–W and its composites, since when using a lower magnification, the surface appeared to have no growth at all. FE-SEM of pure PE demonstrated that it did not cause a bioactive response when placed *in vitro*. Apatite was seen to form on all the other samples that

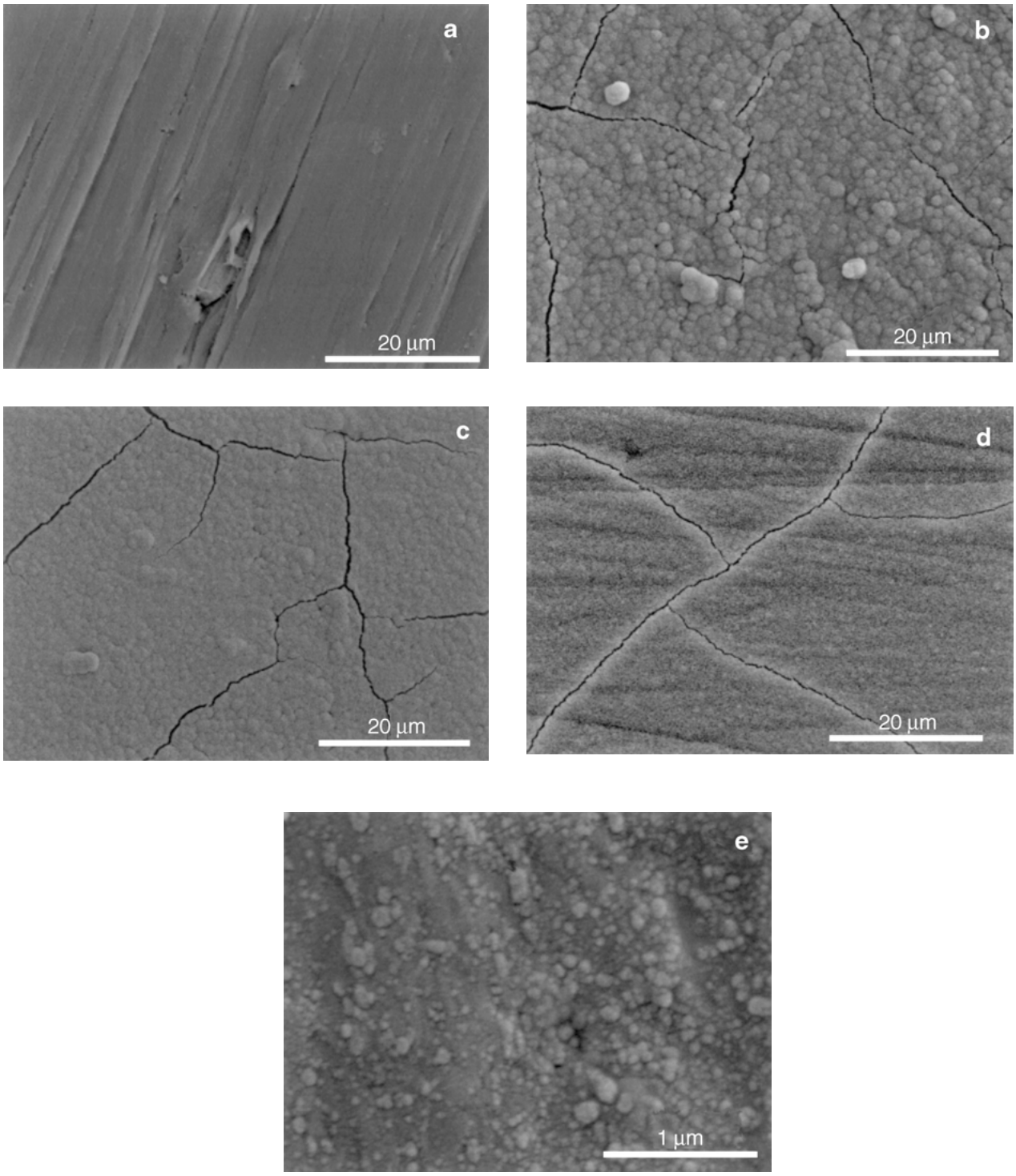

Figure 4 Apatite formation on samples immersed in SBF for one day; AWPEX-10 (a), AWPEX-40 (b), AWPEX-50 (c), pure glass-ceramic A–W (d), and HAPEX™ (e).

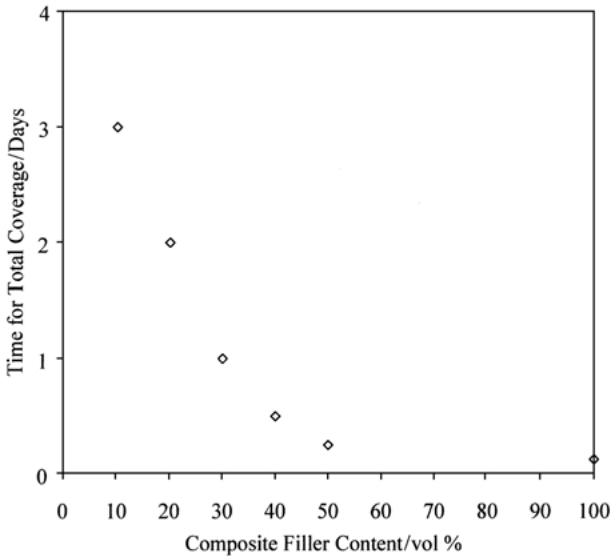

Figure 5 Graphical representation of the time taken for total apatite coverage.

contained glass-ceramic A–W and HA. With increasing SBF immersion time, the apatite layer that was detected showed an increase in crystallinity, indicated by the increase in peak height due to the apatite phase. As the immersion time increased to 7 days, the main apatite phase peaks at the 211, 112, 300, and 002 planes, were found to become broader. The apatite layer formed on the AWPEXs with 40 and 50 vol % glass-ceramic A–W content demonstrated a similar rate of apatite growth to that observed on samples of pure glass-ceramic A–W. It was found that with increased filler content the number of sites available for apatite nucleation increased, hence increasing the overall growth and coverage that could be achieved. Therefore, with increased filler content, the time taken for total sample coverage to be achieved decreased (Fig. 5).

Fig. 6 shows the changes in calcium, phosphate, magnesium, and silicon ion concentrations in SBF with immersion time for AWPEX-30, -40, and -50, pure glass-ceramic A–W, and HAPEX™.

The levels of magnesium ion concentration in the SBF did not alter significantly with time and remained at approximately 1.5 mM for all samples although pure glass-ceramic A–W and AWPEX-50, indicated a slight increase as the materials released magnesium ions into the surrounding fluid. However, a marked decrease in both the calcium and phosphorus ion concentrations was observed. Simultaneously with these decreases and the formation of the apatite layer, an increase in the concentration of silicon ions was observed in the SBF.

Overall, the rate of calcium and phosphorus ion concentration decrease (i.e. the consumption of these ions for apatite formation) occurred in the following sequence: AWPEX-50 > AWPEX-40 > AWPEX-30. Closer observation of the calcium ion concentrations demonstrated a slight increase occurring for glass-ceramic A–W and AWPEX-40 and -50 after 1 day immersion in SBF, where AWPEX-30 and HAPEX™ consumed calcium from zero time point causing a steady decrease in the calcium ion concentration of the SBF. An appreciable amount of silicon ions were detected in the SBF for all the AWPEX samples tested. The rate of

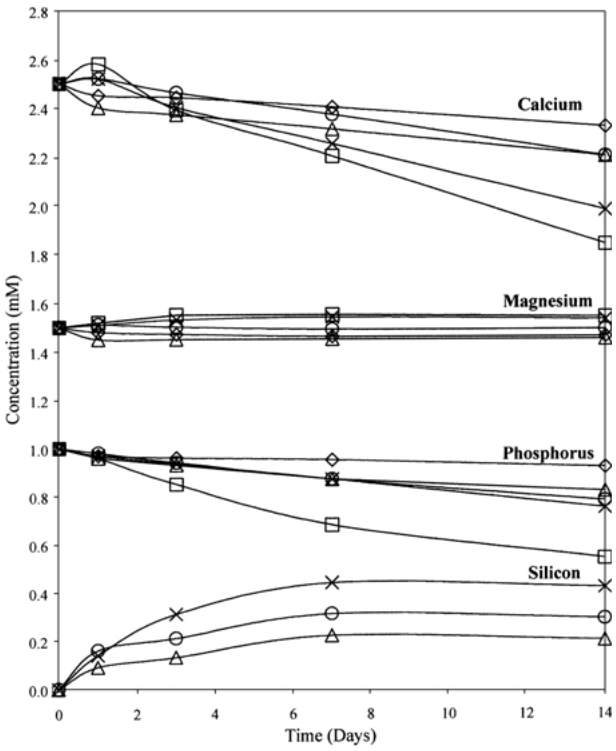

Figure 6 Variation in calcium, phosphorus, magnesium, and silicon ion concentrations of SBF with increasing soaking time of AWPEX (△ = 30 vol %, ○ = 40 vol %, × = 50 vol %), HAPEX™ (◇), and pure glass-ceramic A–W (□) samples.

increase in silicon ion concentration, which implied the release of silicon from the samples, increased with increasing filler content, i.e. AWPEX-30 > AWPEX-40 > AWPEX-50.

4. Discussion

The results showed that a homogeneous distribution of glass–ceramic A–W was achieved in all the composites, a factor that is important for optimal mechanical and bioactive properties. The SBF results demonstrated that apatite formed on the entire surface of all composites after only 1 day immersion. The decreases in wollastonite and PE intensities and the increases in the major apatite peaks occurred at a faster rate as the filler content was increased. Once apatite nuclei are formed, they spontaneously grow by consuming the calcium and phosphate ions from the fluid, since it is already supersaturated with respect to the apatite, as the ICP-AES results demonstrated. The broadening of the major apatite peaks with increasing SBF immersion time is characteristic of low crystallinity apatite, which is known to form on the surface of pure glass-ceramic A–W *in vivo* [19, 20] and is due to small crystallites and/or defective structures. Detailed characterization indicated that this apatite layer consisted of small crystallites subtly different in composition and structure to synthetic HA; the apatite being structurally defective, deficient in calcium, and containing carbonate as seen in natural bone [20]. The method of apatite formation on the AWPEX samples can be explained considering the mechanism by which apatite forms on the surface of pure glass-ceramic A–W in SBF. As the ICP-AES results demonstrated, glass-ceramic A–W, whether in the

composite or in the monolithic form, released appreciable amounts of calcium ions into the SBF immediately on immersion. However, this was neither observed at 30 vol % filler, nor for HAPEX™. From previous work by Kokubo *et al*. [21], the release from glass–ceramic A–W is as expected, since on immersion, the calcium ions further increase the degree of supersaturation of the surrounding fluid with respect to apatite [21]. Simultaneously, phosphate ions are consumed by all the composites and the pure glass-ceramic A–W as the apatite layer is formed – these ions, necessary for forming the apatite layer, only being supplied by the surrounding SBF. During these elemental changes, silicon was detected in the SBF for the AWPEX samples. This is as expected, since the glassy and wollastonite phases within the glass-ceramic A–W filler release silicon ions into the surrounding SBF [21]. The release of silicate ions has a role in the formation of apatite in the bone of mammals [21, 22] and has been shown to provide favorable sites for nucleation of the apatite on the surface of glass-ceramic A–W [21, 23] as well as other substrates such as metals and organic polymers [24–26]. The work performed by Takadama *et al*. [24] demonstrated that by a simple biomimetic model system, the method of silanol groups inducing apatite formation in the body could be explained. The silicate ions, with silanol groups available for bonding, were released from the bioactive glass and attached to a collodion film. These groups were then able to combine with calcium ions to form a calcium silicate, which bonded with phosphate ions in the SBF to form an amorphous calcium phosphate that eventually transformed into crystalline apatite with a higher Ca/P ratio of 1.67 – that of bone-like apatite. Research by Miyaji *et al*. [25] also showed that silicate ions were released and could be absorbed onto the surface of the polymerized composite surface and induce apatite formation. Tanahashi *et al*. [26] showed how apatite could form on the surface of organic polymers by a biomimetic process. Among the polymers tested was PE which showed apatite formation via the attachment of silicate groups, but the bonding of this apatite layer was relatively low compared to that of other surfaces such as poly(ethylene terephthalate) (PET), since PE could only bond to the apatite by weak van der Waals forces. These findings demonstrate that in the composites studied in the current investigation, the silicate ions are released from the glassy and wollastonite phases of the filler glass-ceramic A–W and attach to the surface of the PE matrix. These ions induce apatite nuclei to form on the surface of the bioinert matrix as well as on the bioactive filler, causing the bond within the apatite layer to be stronger, as well as the bond strength between the apatite layer and the composite to be increased due to more points of bonding. This mechanism may also have operated for AWPEX-10 and -20 allowing for a continuous surface apatite layer to be formed after 3

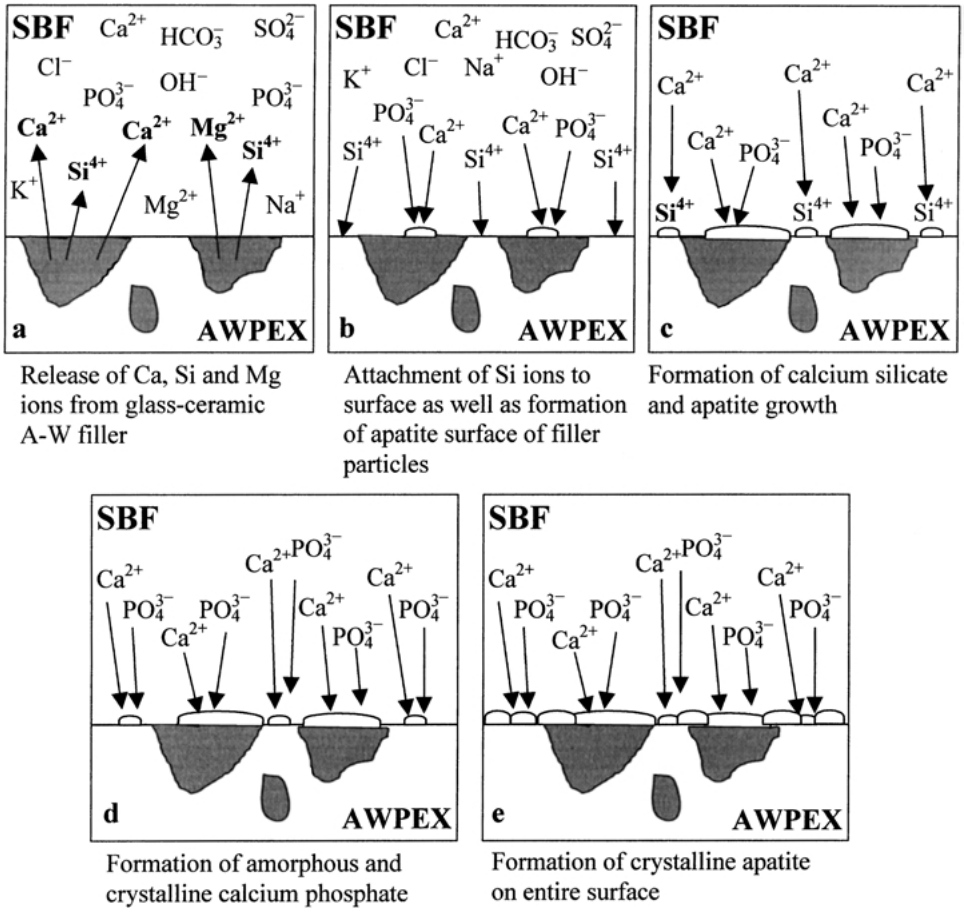

Figure 7 Apatite formation on AWPEX when immersed into SBF. An initial release of calcium, silicon and magnesium ions into the surrounding SBF takes place (a) followed by the growth of apatite on the glass-ceramic A–W particles and the attachment of silicon to the composite surface (b). Due to the attachment of the silicon ions, a calcium silicate can form on the surface of the sample (c) which can in turn attract phosphate groups, creating amorphous calcium phosphates (d), and then the eventual coverage of the entire surface with crystalline apatite (e). The Si^{4+} would be in the form of $H_2SiO_4^{2-}$, $HSiO_4^{2-}$ or $H_2SiO_4^{-}$ in the SBF once released from the AWPEX samples.

days of immersion. Therefore, the mechanism of apatite formation on AWPEX (with greater glass-ceramic A–W filler contents) can be described as shown in Fig. 7, which shows the initial release of calcium, silicon, and some magnesium ions into the surrounding SBF followed by the growth of apatite on the glass-ceramic A–W particles and the attachment of silicon to the composite surface. Due to the attachment of the silicon ions, a calcium silicate can form on the surface of the sample, which can in turn attract phosphate groups, creating amorphous calcium phosphates, and then the eventual coverage of the entire surface with crystalline apatite.

Comparing AWPEX-40 with HAPEX™, demonstrated that AWPEX would potentially provide a stronger bond of the apatite layer with the substrate due to the silicate ion attachment to the polymer. The smaller particles of the glass-ceramic A–W were able to fill the gaps created by the larger particles, which permitted a greater bioactive surface area to be exposed and, hence, greater dissolution of calcium and silicate ions into the surrounding SBF to occur. This effect increased the rate of apatite nucleation and growth more than that seen on HAPEX™ where no dissolution of the HA particles takes place, hence, slowing the formation of apatite. The nodular nature of the HA particles also resulted in less bioactive surfaces being exposed to the SBF from the matrix polymer compared to the dense, angular glass-ceramic A–W particles.

5. Conclusions

All the AWPEX samples tested in this study were able to induce the formation of an apatite layer. The composites with 40 and 50 vol % filler content achieved this result in a much shorter space of time of less than 1 day, comparable to that observed on pure glass-ceramic A–W. As well as pure glass-ceramic A–W, the AWPEX samples with 30, 40 and 50 vol % filler content initially released calcium and silicon ions, helping to increase the rate of apatite formation. Overall, the results of the present bioactivity investigations demonstrate that, the composite AWPEX-50 is the most promising for use as an implant material.

Acknowledgments

The authors would like to thank Nippon Electric Glass Co., Japan, for supplying particulate glass-ceramic A–W. Thanks also to Dr W. McGregor and Prof. K. E. Tanner. (both at the IRC in Biomedical Materials, London, England) for production of all composites. Thanks also to Ms P. Jha and Mr M. Greaves of the Department of Earth Sciences, University of Cambridge, for help with the ICP-AES testing. Support from the UK EPSRC is gratefully acknowledged as is the scholarship provided by YKK (UK) Ltd. enabling J. A. Juhasz to continue research in Japan.

References

1. T. KOKUBO, M. SHIGEMATSU, Y. NAGASHIMA, M. TASHIRO, T. NAKAMURA, T. YAMAMURO and S. HIGASHI, *Bull. Inst. Chem. Res., Kyoto Univ.* **60** (1982) 260.
2. M. JARCHO, C. H. BOLEN, M. B. THOMAS, J. BOBICK, J. F. KAY and R. H. DOREMUS, *J. Mater. Sci.* **11** (1976) 2027.
3. D. M. LIU and H. M. CHOU, *J. Mater. Sci.: Mater. Med.* **5** (1994) 7.
4. T. KOKUBO, *Biomater.* **12** (1991) 155.
5. A. RAVAGLIOLI, A. KRAJEWSKI and G. DE PORTU, in ''Bioceramics 1'', edited by H. Oonishi, H. Aoki and K. Sawai (Ishiyaku EuroAmerica, Inc., Tokyo, 1989) p. 13.
6. J. Y. RHO, R. B. ASHMAN and C. H. TURNER, *J. Biomech.* **26** (1993) 111.
7. J. C. BEHIRI and W. BONFIELD, *ibid.* **17** (1984) 25.
8. T. YAMAMURO, in ''Bioceramics 8'', edited by J. Wilson, L. L. Hench and D. C. Greenspan (Elsevier Science Ltd., Oxford, 1995) p. 123.
9. T. YAMAMURO, in ''Handbook of Bioactive Ceramics, Bioactive Glasses and Glass-ceramic, Vol. 1'', edited by T. Yamamuro, L. L. Hench and J. Wilson (CRC Press, Boca Raton, 1990) p. 335.
10. T. NAKAMURA, T. YAMAMURO, S. HIGASHI, T. KOKUBO and S. ITO, *J. Biomed. Mater. Res.* **19** (1985) 685.
11. T. KOKUBO, S. ITO, M. SHIGEMATSU, S. SAKKA and T. YAMAMURO, *J. Mater. Sci.* **22** (1987) 4067.
12. W. BONFIELD, J. A. BOWMAN and M. D. GRYNPAS (1984), UK Patent 2,085,461B.
13. W. BONFIELD, J. A. BOWMAN and M. D. GRYNPAS (1991) US Patent 5,017,627.
14. K. E. TANNER, R. N. DOWNES and W. BONFIELD, *Brit. Ceram. Trans.* **93** (1994) 104.
15. W. BONFIELD, in ''Annals of the New York Academy of Sciences'', edited by P. Ducheyne and J. E. Lemons (New York Academy of Sciences, New York, 1988) p. 173.
16. M. WANG, T. KOKUBO and W. BONFIELD in ''Bioceramics 9'', edited by T. Kokubo, T. Nakamura and F. Miyaji (Elsevier Science Ltd., Oxford, 1996) p. 387.
17. T. KOKUBO, H. KUSHITANI, S. SAKKA, T. KITSUGI and T. YAMAMURO, *J. Biomed. Mater. Res.* **24** (1990) 721.
18. M. WANG, D. PORTER and W. BONFIELD, *Brit. Ceram. Trans.* **93** (1994) 91.
19. T. KITSUGI, T. YAMAMURO, T. NAKAMURA, S. HIGASHI, Y. KAKUTANI, K. HYAKUNA, S. ITO, T. KOKUBO, M. TAKAGI and T. SHIBUYA, *J. Biomed. Mater. Res.* **20** (1986) 1295.
20. T. KITSUGI, T. NAKAMURA, T. YAMAMURO, T. KOKUBO, T. SHIBUYA and T. TAKAGI, *ibid.* **21** (1987) 1255.
21. T. KOKUBO, H. KUSHITANI, C. OHTSUKI, S. SAKKA and T. YAMAMURO, *J. Mater. Sci.: Mater. Med.* **3** (1992) 79.
22. E. M. CARLISLE, *Science* **167** (1970) 279.
23. T. KOKUBO, *J. Non-Cryst. Solids* **120** (1990) 138.
24. H. TAKADAMA, H.-M. KIM, F. MIYAJIM, T. KOKUBO and T. NAKAMURA, *J. Ceram. Soc. Jpn.* **108** (2000) 118.
25. F. MIYAJI, Y. MORITA, T. KOKUBO and T. NAKAMURA, *ibid.* **106** (1998) 465.
26. M. TANAHASHI, T. YAO, T. KOKUBO, M. MINODA, T. MIYAMOTO, T. NAKAMURA and T. YAMAMURO, *J. Am. Ceram. Soc.* **77** (1994) 2805.

Received 20 April
and accepted 22 August 2002